

# PROMPT OPTICAL EMISSION FROM RESIDUAL COLLISIONS IN GRB OUTFLOWS

ZHUO LI<sup>1</sup> AND ELI WAXMAN<sup>1</sup>

*Draft version February 2, 2008*

## ABSTRACT

The prompt  $\gamma$ -ray emission in  $\gamma$ -ray bursts is believed to be produced by internal shocks within a relativistic unsteady outflow. The recent detection of prompt optical emission accompanying the prompt  $\gamma$ -ray emission appears to be inconsistent with this model since the out flowing plasma is expected to be highly optically thick to optical photons. We show here that fluctuations in flow properties on short,  $\sim 1$  ms, time scale, which drive the  $\gamma$ -ray producing collisions at small radii, are expected to lead to "residual" collisions at much larger radii, where the optical depth to optical photons is low. The late residual collisions naturally account for the relatively bright optical emission. The apparent simultaneity of  $\gamma$ -ray and optical emission is due to the highly relativistic speed with which the plasma expands. Residual collisions may also account for the X-ray emission during the early "steep decline" phase, where the radius is inferred to be larger than the  $\gamma$ -ray emission radius. Finally, we point out that inverse-Compton emission from residual collisions at large radii is expected to contribute significantly to the emission at high energy, and may therefore "smear" the pair production spectral cut-off.

*Subject headings:* acceleration of particles — magnetic fields — shock waves — gamma-rays: bursts

## 1. INTRODUCTION

In the leading model for  $\gamma$ -ray bursts (GRBs), the energy source is a compact object that drives a relativistic unsteady outflow with fluctuating Lorentz factor. Internal shocks within the outflow dissipate the bulk kinetic energy and produce  $\gamma$ -rays (Rees & Meszaros 1994; Paczynski & Xu 1994). A substantial fraction of the outflow kinetic energy may be dissipated in this model outside the photosphere, allowing one to account for the non-thermal spectra and for the complicated light curves of GRBs (Kobayashi et al. 1997). The internal shocks are expected to generate/amplify magnetic fields and to accelerate electrons, which produce MeV  $\gamma$ -rays by synchrotron emission (For review of internal shock models, see Waxman 2003).

Due to the relatively short duration of the prompt  $\gamma$ -ray emission,  $T \sim 1$  to  $10^2$  s, the observation of long-wavelength (optical) prompt emission is a difficult task. GRB 990123 was the first event for which optical emission was detected during the burst (Akerlof et al. 1999). Today, thanks to the rapid localization of GRBs by the *Swift* satellite (see Zhang 2007, for recent review), a larger number of optical (and longer wavelengths) observations are carried out during the bursting phase (e.g. Blake et al. 2005; Vestrand et al. 2005, 2006; Yost et al. 2007).

As shown in § 2 (see also Li & Song 2004), during the emission of prompt  $\gamma$ -rays the plasma is expected to be optically thick to optical photons due to strong synchrotron self-absorption. This appears to be inconsistent with the detection of bright optical emission accompanying  $\gamma$ -ray emission. We point out here that the internal collisions at small radii, which produce the  $\gamma$ -ray emission, are expected to lead to "residual" collisions at much larger radii, where the optical depth to optical photons is low. These late residual collisions may nat-

urally account for the relatively bright optical emission. The apparent simultaneity of  $\gamma$ -ray and optical emission is due to the highly relativistic speed with which the plasma expands. The time delay between  $\gamma$ -ray and optical emission is expected to be shorter than a second, too short to be identified by current optical observations which usually have lower temporal resolution. We discuss in §3 residual collisions in unsteady outflows, and derive the long-wavelength emission they are expected to produce at large radii. The implications of our results are discussed in § 4.

## 2. STRONG SYNCHROTRON ABSORPTION AT SMALL RADII

We first show that during the prompt  $\gamma$ -ray emission phase the plasma is highly optically thick to optical photons. Consider a relativistic outflow with a Lorentz factor fluctuating over a timescale  $t_{\text{var}}$ . We denote the mean Lorentz factor by  $\Gamma$ , its variance by  $\sigma_\Gamma^2$ , and assume  $\sigma_\Gamma \lesssim \Gamma$ . The internal collisions that produce  $\gamma$ -rays occur in this model at a radius  $R_\gamma \sim \Gamma^3 c t_{\text{var}} / \sigma_\Gamma \approx 10^{12.5} (\Gamma / \sigma_\Gamma) \Gamma_{2.5}^2 t_{\text{var}, -3} \text{cm}$ , where  $\Gamma_{2.5} = \Gamma / 10^{2.5}$ , and  $t_{\text{var}, -3} = t_{\text{var}} / 10^{-3} \text{s}$ . The observed variability time implies  $R_\gamma \lesssim 10^{14} \Gamma_{2.5}^2 \text{cm}$  for a large fraction of BATSE bursts (Woods & Loeb 1995). We assume that internal collisions lead to shocks that generate/amplify magnetic fields and accelerate electrons to high energy, leading to synchrotron emission that accounts for the prompt  $\gamma$ -rays.

For typical outflow parameters, the cooling time of the electrons,  $t_c$ , is short compared to the dynamical time,  $t_d$ , over which the plasma expands. The dynamical time measured in the plasma frame is  $t_d \sim R / \Gamma c \sim 1 R_{13} / \Gamma_{2.5} \text{s}$ , where  $R_{13} = R / 10^{13} \text{cm}$ . The cooling time of electrons with Lorentz factor  $\gamma_\nu$ , emitting synchrotron photons of frequency  $\nu$ , is  $t_c \approx \gamma_\nu m_e c^2 / P_{\text{syn}} (1+y)$ , where  $P_{\text{syn}} = (4/3) \sigma_T c \gamma_\nu^2 B^2 / 8\pi$  and  $y \equiv P_{\text{IC}} / P_{\text{syn}}$  is the ratio between inverse-Compton and synchrotron emission, which is roughly given by the ratio of radiation and mag-

<sup>1</sup> Physics Faculty, Weizmann Institute of Science, Rehovot 76100, Israel

netic field energy densities,  $U_\gamma/(B^2/8\pi)$ . In order to account for the  $\gamma$ -ray emission, the magnetic field energy density needs to be close to equipartition with the thermal energy of the plasma. Since a significant fraction of this thermal energy is emitted as  $\gamma$ -rays, we estimate  $B^2/8\pi \sim U_\gamma$ . Using  $U_\gamma \simeq L_\gamma/4\pi R_\gamma^2 \Gamma^2 c$  this gives  $B \sim 10^5 L_{\gamma,51}^{1/2} \Gamma_{2.5}^{-1} R_{13}^{-1}$  G and  $t_c \sim 10^{-2} \Gamma_{2.5} / B_5 \nu'_{15} (1+y)s$ , where  $L_{\gamma,51} = L_\gamma/10^{51} \text{erg s}^{-1}$ ,  $B_5 = B/10^5$  G, and  $\nu'_{15} = \nu'/10^{15}$  Hz is the observed frequency,  $\nu' = \Gamma\nu = \Gamma\gamma_\nu^2 eB/2\pi m_e c$ . Since  $t_c(\nu'_{15} = 1) \ll t_d$ , the electrons, which were initially accelerated to high energy at which their synchrotron emission peaks at  $\sim 1$  MeV, rapidly cool down to energies at which their synchrotron emission peaks well below the optical band. Neglecting synchrotron self-absorption, this would have lead to a synchrotron spectrum of  $F_\nu \propto \nu^{-1/2}$  extending from the  $\gamma$ -ray band to below the optical band ( $F_\nu$  stands for the flux per unit frequency).

Self-absorption of photons of frequency  $\nu$  is dominated by electrons with Lorentz factor  $\gamma_\nu$ , which constitute a fraction  $t_c(\gamma_\nu)/t_d$  of the electron population. We may therefore approximate the (volume averaged) absorption coefficient by  $\alpha_\nu \approx n_e [t_c(\gamma_\nu)/t_d] e^3 B/2\gamma_\nu (m_e c \nu)^2$ , where the electron density is given by  $n_e = L_k/4\pi \Gamma^2 R^2 m_p c^3$ , with  $L_k$  the kinetic luminosity of the GRB outflow. The self-absorption frequency, where the optical depth  $\alpha_\nu R/\Gamma$  equals unity, is

$$h\nu'_a \approx 0.3 L_{k,52}^{1/3} \Gamma_{2.5}^{1/3} R_{13}^{-2/3} (1+y)^{-1/3} \text{keV}, \quad (1)$$

independent of  $B$ , and the corresponding electron Lorentz factor is  $\gamma_a \equiv \gamma_\nu(\nu_a) \approx 30 L_{k,52}^{1/6} \Gamma_{2.5}^{-1/3} B_5^{-1/2} R_{13}^{-1/3} (1+y)^{-1/6}$ . Here  $L_{k,52} = L_k/10^{52} \text{erg s}^{-1}$ . Note, that the electron cooling rate is modified below  $\gamma_a$ , and  $t_c$  becomes larger than that used for deriving eq. (1), due to the absorption of radiation. However this modification is not large for  $y \sim 1$ , in which case cooling by inverse-Compton emission is comparable to synchrotron cooling.

Examining eq. (1), we expect a large optical depth below the X-ray band and hence a strong suppression of the optical flux. This appears to be inconsistent with observations, which typically show  $F_{\nu_{\text{op}}} \gtrsim F_{\nu_\gamma}$  (e.g., Yost et al. 2007). It should be mentioned here that, within the context of the current model, the constraint  $R_\gamma < 10^{14}$  cm, which implies  $\nu'_a \gg 1$  eV, is obtained not only from the observed variability time,  $t_{\text{var}}$ , but also from the requirement that the synchrotron emission peaks in the MeV band. The characteristic (plasma frame) Lorentz factor of the  $\gamma$ -ray emitting electrons is  $\gamma_e \sim m_p/m_e$  (see § 3.2), leading to synchrotron emission peaking at

$$h\nu'_p \approx \hbar \Gamma \gamma_e^2 \frac{eB}{m_e c} \approx 0.3 L_{\gamma,51}^{1/2} R_{13}^{-1} \text{MeV}. \quad (2)$$

$h\nu'_p \sim 1$  MeV implies therefore  $R_\gamma \lesssim 10^{13}$  cm. This constraint may be avoided, for bursts where  $R_\gamma \lesssim 10^{13}$  cm can not be inferred from  $t_{\text{var}}$ , in a model where  $\gamma$ -ray emission is assumed to be produced by inverse-Compton scattering of  $h\nu'_p \ll 1$  MeV synchrotron photons (assuming magnetic field well below equipartition). In such a model the inverse-Compton spectrum is expected to be hard,  $F_\nu \propto \nu^2$ , at low frequencies,  $h\nu' < 1$  MeV,

due to self-absorption of the synchrotron spectrum (e.g. Panaitescu & Mészáros 2000). The observed spectrum is softer for most bursts.

### 3. LARGE-RADIUS EMISSION FROM RESIDUAL COLLISIONS

The optical depth for optical photons drops below unity at radii  $R \gtrsim 10^{15}$  cm (see eq. 1; note  $(1+y) \propto R^{2/3}$ , see §3.2). We show here that the optical emission could be produced by "residual" collisions at such large radii. Note, that the time delay between  $\gamma$ -ray and optical emission in this model,

$$\tau_{\text{delay}} \approx R_{\text{op}}/2\Gamma^2 c \sim 0.2 R_{\text{op},15} \Gamma_{2.5}^{-2} s, \quad (3)$$

is expected to be shorter than the characteristic temporal resolution of the optical observations, which is a few seconds. Thus, optical and  $\gamma$ -ray emission may appear to be simultaneous. However, better temporal resolution may allow one to detect a systematic time delay between the two wave bands. In addition, one would expect larger observed variability timescales at longer wavelengths,  $t_{\text{var,op}} \sim \tau_{\text{delay}}$ .

We approximate the outflow by a sequence of  $N \gg 1$  equal mass shells ( $i = 1, \dots, N$ ) separated by an initial fixed distance  $ct_{\text{var}}$  and expanding with (initial) Lorentz factors  $\Gamma_{i,0}$  drawn from a random distribution with an average  $\Gamma$  and initial variance  $\sigma_{\Gamma,0}^2 < \Gamma^2$ . We assume that the radial extent of the outflow  $Nct_{\text{var}}$  is much smaller than the collision radii  $R > \Gamma^2 ct_{\text{var}}$ , i.e.  $N \ll \Gamma^2$ , which is reasonable given the observed variability (e.g. Fishman & Meegan 1995). The model may, of course, be complicated, e.g. by adding several variability times or by allowing variable mass shells. Adding such degrees of freedom may allow one to control the details of the predicted long wave length emission. Our main goal is to demonstrate that the simplest model considered here may naturally account for the observed optical emission.

The dynamics of late residual collisions is discussed in § 3.1, and the radiation they are expected to generate is discussed in § 3.2.

#### 3.1. Late residual collisions

Let us first consider the evolution of the outflow using the simplifying assumption that shells merge after collisions. This assumption would be approximately valid if all the internal energy generated by a collision of two shells is radiated away. As the flow radius increases, the typical number  $n(R)$  of initial shells that merge into one single shell increases, and the variance of the Lorentz factors of the resulting shells decreases. For a group of shells with a small Lorentz factor variance, the velocities  $v_i$  of the shells in the shells' center of momentum frame are not highly relativistic. In this case, conservation of momentum implies that the velocity of a merged group of shells is given by the average of merged shells' velocities,  $\bar{v} = (1/n) \sum_{i=1}^n v_i$ , and that the variance of the velocities of merged groups of shells is  $\sigma_v(n) = \sigma_{v,0}/\sqrt{n}$  where  $\sigma_{v,0}$  is the initial variance. This, in turn, implies that the variance of (observer frame) Lorentz factors,  $\sigma_\Gamma(n)/\Gamma \approx \sigma_v(n)/c$ , evolves like  $\sigma_\Gamma(n) = \sigma_{\Gamma,0}/\sqrt{n}$ . Collisions of merged groups of  $n$  shells will therefore take place at a radius  $R(n) \sim \Gamma^3 c \times nt_{\text{var}}/\sigma_\Gamma(n)$ , which implies

$$n \propto R^{2/3}, \quad \sigma_v \propto \sigma_\Gamma \propto R^{-1/3}. \quad (4)$$

The outflow energy that may be dissipated and radiated away is the energy associated with the random velocities of the shells (in the outflow rest frame). This energy decreases as

$$E_{\text{fluc}} \propto \Gamma \sigma_v^2 \propto R^{-2/3}. \quad (5)$$

Let us consider next the evolution of the outflow dropping the assumption of shell merger. In order to describe the evolution in this case we carried out a numerical simulation, assuming that in each collision one third of the kinetic energy of the two shells (in the center of momentum frame) is radiated away, and that the shells separate after the collision, each carrying half the remaining energy (in the center of momentum frame). Fig. 1 shows the evolution of an outflow with the following parameters:  $N = 10^3$ ,  $t_{\text{var}} = 1$  ms and  $\Gamma_i = 10^{2.5} \times 3^\xi$  with  $\xi$  normally distributed with zero mean and unit standard deviation. As can be seen from the top two panels of the figure, the evolution of  $\sigma_v$  and of the radiated energy are well approximated by the analytic expressions of eq. (4) and (5), which were obtained under the shell merger assumption. We will therefore use these approximate analytic expressions in the next section, where the emitted radiation is discussed.

### 3.2. Predicted emission

Let us first consider the energy band into which energy is radiated. We make the common assumptions, that internal shocks accelerate electrons and generate or amplify magnetic fields, such that the post-shock electrons and magnetic fields carry fixed fractions,  $\epsilon_e$  and  $\epsilon_B$  respectively, of the post-shock internal energy. Under these assumptions, the characteristic Lorentz factor of post-shock electrons (in the outflow co-moving frame) scales as  $\gamma_i \propto \epsilon_e \sigma_v^2$ , and the post-shock magnetic field scales as  $B^2 \propto \epsilon_B \sigma_v^2 n_e$  (the particle number density scales as  $n_e \propto R^{-2}$ ). Using eq. (4), the characteristic (observer frame) frequency of synchrotron photons,  $\nu_i \propto \Gamma_i^2 B$ , scales as

$$\nu_i \propto \sigma_v^5 R^{-1} \propto R^{-8/3}. \quad (6)$$

As can be seen in the bottom panel of fig. 1, eq. (6), which is based on the analytic approximations of eq. (4) for the simplified "merging-shell" model, describes well also the results of the numerical simulation for the non-merging model.

Next, consider the emitted flux. It is straight forward to show that the cooling time of the electrons is short compared to the dynamical time during the late residual collision phase, up to radii  $R \sim 10^3 R_\gamma$ . We therefore assume that electrons radiate away all their energy. During the phase of late residual collisions, the plasma is immersed in the radiation bath of the prompt  $\gamma$ -rays. The radiation energy density dominates the magnetic field energy density, since the photon energy density drops as  $U_\gamma \propto R^{-2}$  and the ratio  $y = U_\gamma / (B^2 / 8\pi) \propto \sigma_v^{-2} \propto R^{2/3}$  increases with  $R$ . The electrons lose therefore most of their energy by IC cooling, and only a fraction  $1/(1+y) \approx y^{-1} \propto R^{-2/3}$  of the radiated energy is emitted as synchrotron radiation. Neglecting synchrotron self-absorption, the observed (time-integrated) spectrum would be  $\nu F_\nu \propto E_{\text{fluc}} y^{-1}|_{\nu_i=\nu} \propto R^{-4/3}|_{\nu_i=\nu} \propto \nu^{1/2}$ .

Finally, let us consider the effects of synchrotron self-absorption. Eq. (1) is valid for  $\nu_a < \nu_i$ , which implies

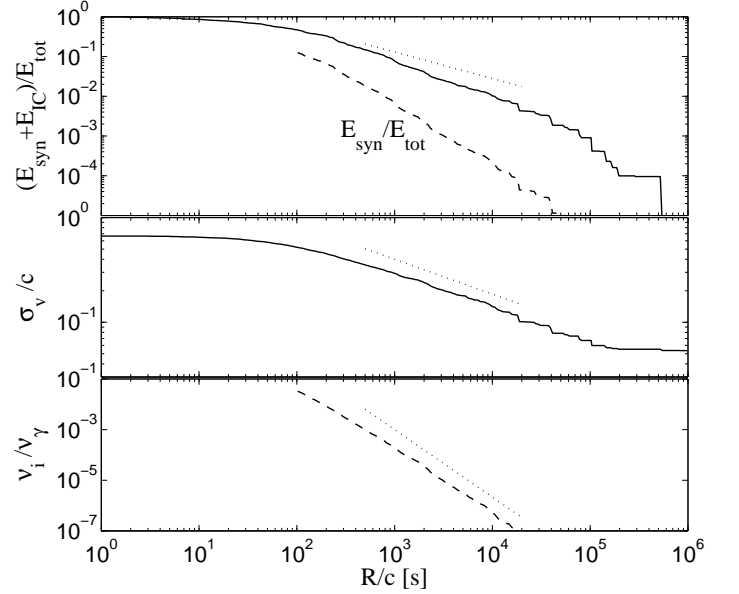


FIG. 1.— The evolution of an outflow composed of  $N = 10^3$  equal mass shells initially separated by  $ct_{\text{var}} = c \times 1$  ms, with random Lorentz factors  $\Gamma_i = 10^{2.5} \times 3^\xi$  where  $\xi$  is normally distributed with zero mean and unit standard deviation. In each collision it is assumed that 1/3 of the internal energy generated is radiated (see § 3.1 for more details). *Top panel:* The energy radiated by collisions at radii larger than  $R$ , normalized to the total radiated energy (solid line- synchrotron and IC emission, dashed line- synchrotron emission only); *Middle panel:* The standard deviation of shell velocities (in the center of momentum frame) as function of  $R$ ; *Bottom panel:* The characteristic frequency of synchrotron radiation (see § 3.2) as a function of  $R$ , normalized to its value at the smallest collision radius. Dotted lines show the approximate analytic scaling laws obtained for the "merging-shell" model (eqs. 4, 5, 6).  $\sim 1\%$  of the radiated energy is released at a radius  $R/c \sim 10^4$  s, where residual collisions produce optical synchrotron photons,  $\nu_i/\nu_\gamma \sim 10^{-6}$ . Most of this energy is emitted by inverse-Compton scattering of the prompt  $\gamma$ -rays.

$\nu_a \propto R^{-2/3} y^{-1/3} \propto R^{-8/9}$ . For  $\nu_a < \nu_i$  we therefore have  $\nu_a/\nu_i \propto R^{16/9}$ , implying that the optical depth to synchrotron photons emitted by electrons with the characteristic Lorentz factor  $\gamma_i$  will exceed unity at sufficiently large radii,  $R > R_{ia}$ . Since at small radii,  $R \sim R_\gamma$ ,  $\nu_i = \nu_\gamma \sim 1$  MeV and  $\nu_a \sim 0.3$  keV (see eq. 1),  $\nu_i = \nu_a$  is obtained at  $R = R_{ia} \sim 10^2 R_\gamma$ . At this radius  $\nu_i = \nu_a = \nu_{ia} \equiv \nu_i(R_{ia}) \sim 10$  eV. Thus, the  $\nu F_\nu \propto \nu^{1/2}$  (time-integrated) spectrum obtained above neglecting self-absorption does not extend down to the optical band. In order to derive the spectrum at lower frequencies,  $\nu < \nu_{ia}$ , we first derive the evolution of  $\nu_a$  at  $R > R_{ia}$ . For these radii one needs to consider the electrons accelerated to Lorentz factors larger than the characteristic Lorentz factor  $\gamma_i$ , since these electrons dominate emission and absorption at  $\nu > \nu_i$ . Shock acceleration is expected to generate a power-law energy distribution of electrons,  $dn_e/d\gamma_e \propto \gamma_e^{-2}$  at  $\gamma_e > \gamma_i$ . For this energy distribution, the volume averaged number density of electrons with Lorentz factor  $\gamma_\nu > \gamma_i$  is  $n_e[t_c(\gamma_\nu)/t_d](\gamma_i/\gamma_\nu) = n_e[t_c(\gamma_\nu)/t_d](\nu_i/\nu)^{1/2}$ . Using the

same argument leading to eq. (1) we find, for  $\nu_a > \nu_i$ ,

$$\nu_a \propto \sigma_v^{9/7} R^{-5/7} \propto R^{-8/7}. \quad (7)$$

The flat electron energy distribution,  $\gamma_e^2 dn_e/d\gamma_e \propto \gamma_e^0$ , generates equal amounts of synchrotron energy in logarithmic photon energy intervals,  $\nu F_\nu \propto \nu^0$  for  $\nu > \nu_a$  (when  $\nu_a > \nu_i$ ). We therefore obtain for  $\nu < \nu_{ia}$  a (time integrated) spectrum given by  $\nu F_\nu \propto E_{\text{fluc}} y^{-1}|_{\nu_a=\nu} \propto R^{-4/3}|_{\nu_a=\nu} \propto \nu^{7/6}$ .

Combining the above results, the observed flux at  $\nu < \nu_{ia}$  is given by

$$\frac{F_\nu}{F_{\nu_\gamma}} \simeq \left( \frac{\nu_{ia}}{\nu_\gamma} \right)^{-1/2} \left( \frac{\nu}{\nu_{ia}} \right)^{1/6} \sim 10^2 \left( \frac{h\nu'}{1 \text{ eV}} \right)^{1/6}. \quad (8)$$

Several comments should be made here. The flux ratio given by eq. (8) holds only on average. The observed flux ratios in individual GRB events may differ significantly, since for a small number of shells (and collisions) large variations in the late residual collisions should be expected. It should also be noticed that we have assumed  $\sigma_{\Gamma,0} < \Gamma$ , while initial conditions with  $\sigma_{\Gamma,0} > \Gamma$  may lead to more efficient  $\gamma$ -ray production at small radii, in which case  $F_\nu/F_{\nu_\gamma}$  should be smaller by a factor of a few than the ratio given in eq. (8).

#### 4. DISCUSSION

We have shown that late residual collisions, that occur at radii much larger than those where  $\gamma$ -ray producing collisions take place, may naturally account for the observed strong optical emission accompanying the prompt GRB. Internal collisions at small radii reduce the variance of colliding shell velocities. As a result, the energy available for radiation at large radii and the characteristic frequency of radiated photons decrease with radius. We find that one may expect optical to  $\gamma$ -ray energy ratio  $\sim 10^{-4}$ , with large burst-to-burst scatter (see fig. 1, eq. 8 and discussion at the end of § 3.2). This is consistent with the results of Yost et al. (2007), who find that during the prompt emission of GRBs the spectral indices between the optical and the  $\gamma$ -ray bands are in the range of  $0 < \beta_{\text{op-}\gamma} < 0.5$ , corresponding to  $F_{\nu_{\text{op}}}/F_{\nu_\gamma} \sim 1 - 10^3$  and implying that the optical emission is only a small fraction,  $\sim 10^{-6} - 10^{-3}$ , of the total emitted energy.

Although the optical emission is produced at large radii, where synchrotron self-absorption is avoided, the expected time delay between  $\gamma$ -ray and optical emission,  $\sim 0.1$  s (see eq. 3), is shorter than the characteristic temporal resolution of the optical observations, which is a few seconds (e.g. Tang & Zhang 2006). Thus, optical and  $\gamma$ -ray emission may appear to be simultaneous. However, better temporal resolution may allow one to detect a systematic time delay between the two wave bands. In addition, one would expect larger observed variability timescales at longer wavelengths,  $t_{\text{var,op}} \sim \tau_{\text{delay}}$ .

Wei (2007) has suggested that optical emission may be generated by strong internal shocks at radii  $R/c > 10^6$  s,

driven by shells emitted with a large time delay,  $\sim 10$  s, following those producing the main  $\gamma$ -ray emission (see also Fan et al. 2005). Our model is quite different. We show that optical emission is naturally expected to arise, without postulating the existence of delayed shells, by residual collisions at  $R/c \sim 10^4$  s, in which the characteristic emitted photon frequency is low,  $h\nu \sim 1$  eV, due to the reduction of the Lorentz factor variance in the flow (rather than by the large radius  $R/c > 10^6$  s). Moreover, we have shown that the optical luminosity can be estimated from the burst  $\gamma$ -ray properties, and that it is consistent with the observations.

The energy released in residual collisions of the relativistic outflow is large. In fact, it would overproduce the optical emission if all the energy is released in the optical band. In the models discussed here, only a small fraction of the energy,  $\sim 10^{-2}$ , is released as synchrotron radiation, since electrons accelerated in residual collisions cool mainly by IC scattering of the prompt GRB  $\gamma$ -rays. This has some important implications to observations at high energy,  $> 100$  MeV. Such observations are expected to be useful in determining the bulk Lorentz factor of GRB outflows and the size of the emitting region by detecting the high energy cutoff due to  $\gamma\gamma$  absorption (e.g., Baring 2000; Lithwick & Sari 2001; Li et al. 2003). The identification of this cutoff may be complicated in the presence of strong high energy emission from residual collisions, that take place at large radii where the  $\gamma\gamma$  optical depth is reduced.

A comment is in place here regarding some recent constraints on the size of the GRB emission region, which were inferred from the early X-ray steep decay. Assuming that the steep decay arises from emission by plasma lying away from our line of sight, large radii were inferred,  $R_{\text{em}} > 2t_{\text{decay}}c/\theta_j^2 \gtrsim 6 \times 10^{13}$  cm for  $t_{\text{decay}} \gtrsim 10^2$  s and  $\theta_j \lesssim 0.3$  (Lazzati & Begelman 2006; Lyutikov 2006; Kumar et al. 2007). Such radii are larger than typically predicted in internal shock models. It should be realized, however, that if the off-the-line-of-sight emission explanation is adopted, the emission during this phase should peak below the X-ray band, and should therefore arise in a region different than that where  $\gamma$ -rays are produced. This is due to the fact that the flat X-ray spectrum ( $F_\nu \propto \nu^0$ ) seen in GRB spectra would imply a light curve decay  $\propto t^{-2}$  (e.g., Kumar & Panaitescu 2000), much shallower than observed (e.g., Tagliaferri et al. 2005). In fact, the spectra during the steep decay are soft, suggesting that indeed the energy peak is below the X-ray band. Thus, if the steep decay is due to off-the-line-of-sight emission, it should originate from a region lying at a larger radius than that where  $\gamma$ -rays are produced, producing emission that peaks below the X-ray band. Such emission may be produced, e.g., by residual collisions.

This research was supported in part by ISF and Minerva grants.

#### REFERENCES

- Akerlof, C., et al. 1999, *Nature*, 398, 400
- Baring, M. G. 2000, American Institute of Physics Conference Series, 515, 238
- Blake, C. H., et al. 2005, *Nature*, 435, 181
- Fan, Y. Z., Zhang, B., & Wei, D. M. 2005, *ApJ*, 628, L25

- Fishman, G. J., & Meegan, C. A. 1995, *ARA&A*, 33, 415
- Kobayashi, S., Piran, T., & Sari, R. 1997, *ApJ*, 490, 92
- Kumar, P., et al. 2007, *MNRAS*, 376, L57
- Kumar, P., & Panaitescu, A. 2000, *ApJ*, 541, L9
- Lazzati, D., & Begelman, M. C. 2006, *ApJ*, 641, 972

- Li, Z., Dai, Z. G., Lu, T., & Song, L. M. 2003, *ApJ*, 599, 380  
Li, Z., & Song, L. M. 2004, *ApJ*, 608, L17  
Lithwick, Y., & Sari, R. 2001, *ApJ*, 555, 540  
Lyutikov, M. 2006, *MNRAS*, 369, L5  
Paczynski, B., & Xu, G. 1994, *ApJ*, 427, 708  
Panaitescu, A., & Mészáros, P. 2000, *ApJ*, 544, L17  
Rees, M. J., & Meszaros, P. 1994, *ApJ*, 430, L93  
Tagliaferri, G., et al. 2005, *Nature*, 436, 985  
Tang, S. M., & Zhang, S. N. 2006, *A&A*, 456, 141  
Vestrand, W. T., et al. 2005, *Nature*, 435, 178  
Vestrand, W. T., et al. 2006, *Nature*, 442, 172  
Waxman, E. 2003, *Supernovae and Gamma-Ray Bursters*, 598, 393  
Wei, D. M. 2007, *MNRAS*, 374, 525  
Woods, E., & Loeb, A. 1995, *ApJ*, 453, 583  
Yost, S. A., et al. 2007, *ApJ*, 669, 1107  
Zhang, B. 2007, *Chinese J. Astron. Astrophys.*, 7, 1